www.czasopisma.pan.pl PAN www.journals.pan.pl

ARCHIVES of FOUNDRY ENGINEERING

ISSN (2299-2944)
Volume 2020
Issue 3/2020

9 – 14

2/3

10.24425/afe.2020.133322

Published quarterly as the organ of the Foundry Commission of the Polish Academy of Sciences

Structure and Mechanical Properties of the CO_2 Laser Welded Joint of AZ91 Cast Magnesium Alloy

A. Dziadoń *, E. Musiał
Kielce University of Technology,
al. Tysiąclecia Państwa Polskiego 7, 25-314 Kielce, Poland
* Corresponding author. E-mail: adziadon@tu.kielce.pl

Received 19.11.2018; accepted in revised form 22.01.2020

Abstract

Plates of AZ91 cast magnesium alloy with a thickness of 3.5 mm were butt-welded using a laser power of 2000 W and helium as the shielding gas. The effect of the welding speed on the weld cross-sectional geometry and porosity was determined by microscopic analysis. It was found that to avoid the formation of macropores, welding should be carried out at a speed of 3.4 m/min or higher. Non-equilibrium solidification of the laser-melted metal causes fragmentation of the weld microstructure. Joints that were welded at optimal laser processing parameters were subjected to structural observations using optical and scanning microscopy and to mechanical tests. The mechanical properties were determined through Vickers hardness measurements in the joint cross-section and through tensile testing. The results indicate that the hardness in the fusion zone was about 20 HV (30%) higher than that of the base material. The weld proved to be a mechanically stable part of the joint; all the tensile-tested specimens fractured outside the fusion zone.

Keywords: AZ91 alloy, Laser welding, Porosity, Microstructure, Mechanical properties

1. Introduction

Magnesium is an attractive material suitable for a variety of structural and mechanical applications primarily because of its low density. It is 36% lighter per unit volume than aluminium and 78% lighter than iron. Hence its application, for instance, in the automotive, aerospace and electronics industries. Almost 90% of components made of magnesium alloys are produced through casting [1, 2]. The oldest and most widely used magnesium alloys are Mg-Al-Zn alloys [3]. One of them is AZ91. It exhibits excellent castability combined with good mechanical properties and acceptable corrosion resistance [1, 4-7]. A wider use of magnesium alloys requires improving their welding process. Over the last twenty years, a number of studies have been devoted to the welding of AZ91 alloy either by gas tungsten arc welding (GTAW) [8-11] or laser welding [12-18]. Generally, laser welding is a high-speed process in which heat is rapidly transported from the weld pool to the surrounding base material. A review of the literature shows that unlike GTAW, laser welding is characterised by low heat input, resulting in a small fusion zone and a narrow heat-affected zone. In addition, laser welding is easy to automate.

Analysis of the literature on the laser welding of AZ91 alloy shows that to date the majority of research in this area has focused on the weld shape and mechanical properties of welded joints. The weld features such as depth of penetration, width, weld reinforcement and surface ripples have generally been determined in relation to the welding parameters [12, 13, 15]. Porosity formation has also been investigated [14, 16, 17]. Laser welding

causes the mechanical properties of the material to change in the fusion zone. Cao [14] reports an increase in the hardness of the fusion zone after welding compared to the hardness of sand-cast AZ91 alloy. Also, microhardness measurements across laser welded joints reveal higher hardness in the fusion zone and the partially melted zone than in the base material [16, 18]. However, there are no clear results regarding the tensile strength of laser welded joints of AZ91. Some research in this area [14] indicates that for die cast AZ91 alloy, the tensile strength of the laser welded joint is of the same order as that of the base material. Other researchers, however, report that both the tensile strength and the yield strength of the material are reduced during welding. For example, Munitz et al. [8], who studied the mechanical properties of gas-welded AZ91 plates, found that the tensile strength of the joint was much lower than that determined for the cast AZ91D ingot.

The different results concerning the strength of welded joints may lead us to question the correctness of the process parameters used in the experiments. Thus, the preliminary objective of this study was to determine the optimal welding conditions. The influence of the welding speed (the speed of the laser beam moving in relation to the workpiece) on the weld microstructure was determined for a constant laser power. Then, it was necessary to select an optimal range of welding speeds that guaranteed the fusion zone free from macropores. The welding of the AZ91 alloy plates was continued at a welding speed selected from this range. This paper provides a detailed analysis of the microstructure of the fusion zone; it also discusses the results of the Vickers hardness measurements and the tensile tests obtained for laser welded joints of AZ91 magnesium alloy.

2. Experimental procedure

Commercial AZ91 magnesium alloy containing 9.11 wt.% Al, 0.64 wt.% Zn and 0.23 wt.% Mn was used in the experiment. The ingot was cut perpendicular to its longitudinal axis to obtain plates 3.5 mm in thickness, 100 mm in length and 50 mm in width. The plates were then cut longitudinally into two halves to be butt welded along the cut line. The welding was carried out using a TRUMPF TLP 6000 CO2 laser system. The specimens (plates) were mechanically clamped into position to weld. Helium, flowing through the nozzle at 10 l/min, was used as the shielding gas. The laser beam diameter was 0.3 mm. A laser power of 2000 W was selected on the basis of the results of the earlier studies. To select the right welding speed, the experiment was performed at speeds ranging from 1.4 m/min to 3.8 m/min with an increment of 0.2 m/min. Further microstructural analysis and strength tests were carried out for welds produced at a constant speed of 3.4 m/min.

The microstructure and Vickers hardness of the welds were determined in the transverse cross-section, perpendicular to the welding direction. The Vickers hardness was measured at a load of 10 kg. Standard metallographic techniques were employed to prepare the specimens for optical and scanning electron microscopy. The optical microscopy (OM) observations were carried out with a METAVAL and a NIKON ECLIPSE MA200, while the scanning electron microscopic (SEM) analysis was performed using a JEOL JSM-5400 equipped with an OXFORD INSTRUMENTS ISIS 300 energy dispersive X-ray analysis system. The tensile tests were conducted using a LAB Test 5.20 SP1 screw-driven machine at an initial strain rate of 4.7 x 10-4sec^{-1}. The tensile properties were measured on specimens with a gauge length of 35 mm, width of 10 mm and thickness of 3.5 mm. The weld was located in the centre of the gauge length. The tensile properties were also determined for the as-cast AZ91 alloy. In both cases four specimens were tensile-tested to failure.

3. Results

3.1. Initial microstructure

Figure 1 shows an OM image of the microstructure of the as-cast AZ91 alloy (AZ91 ingot) used for the welding. As can be seen, there are α-phase dendrites (a solid solution of aluminium in magnesium), which formed at the beginning of the solidification process. The rest of the liquid phase solidified in the interdendritic spaces as a eutectic, which, according to the Mg-Al phase equilibrium system [19], is a mixture of an intermetallic $Mg_{17}Al_{12}$ compound and the α-phase. The dark regions locally visible in the casting microstructure are discontinuous precipitates.

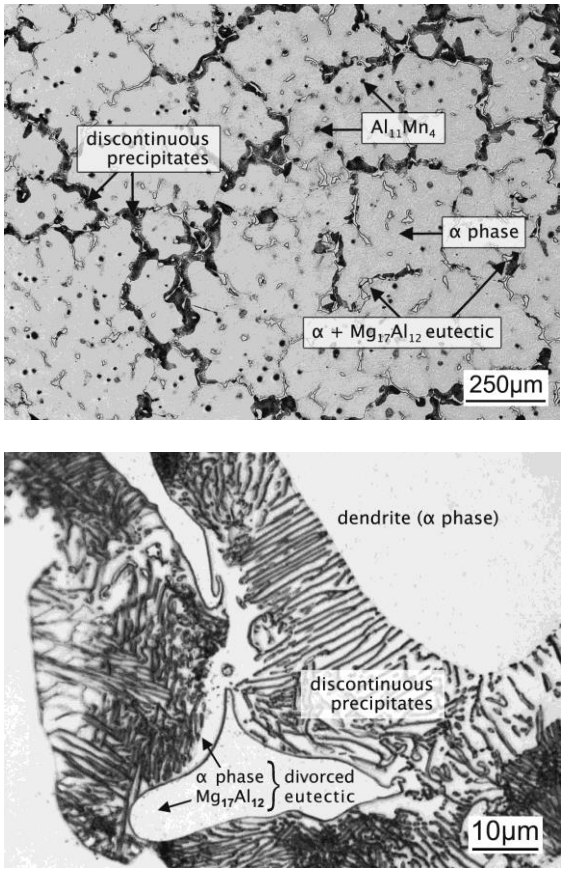

Fig. 1. OM microstructure of the as-cast AZ91 alloy observed at lower (a) and higher (b) magnifications

A higher magnification (Fig. 1b) reveals the microstructure details. Depending on the cooling rate during the solidification, the eutectic can be either partially or fully divorced [20]. The morphology of the eutectic presented in Fig. 1b indicates that it is fully divorced because there are two eutectic phases completely separated (single $Mg_{17}Al_{12}$ particles surrounded by the eutectic α-phase). The lamellar structure adjacent to the eutectic, which is characteristic of discontinuous precipitation, occurs as a result of the decomposition of the solid solution of aluminium in magnesium. Discontinuous precipitation is a cellular growth of the structure with alternating layers of the $Mg_{17}Al_{12}$ and near-equilibrium magnesium matrix phases.

A quantitative EDS analysis was performed to identify the chemical composition of the AZ91 alloy phases. The phase referred to as $Mg_{17}Al_{12}$ contains 61.8 at.% Mg, 36.4 at.% Al and 1.8 at.% Zn. It was also found that the dendrites (a solid solution of aluminium in magnesium) were chemically inhomogeneous. The content of aluminium in the immediate vicinity of the eutectic was in the range of 6 to 7 at.% whereas the content of aluminium in the more distant dendrite region was about 5 at.%. The EDS analysis results obtained for the dendrites indicate also the presence of zinc (approx. 0.2 at.%). The dark, equiaxed particles visible inside the dendrites (Fig. 1a) contain aluminium and manganese. The Al to Mn ratio was 2.72, which suggests the $Al_{11}Mn_4$ phase.

3.2. Microstructure of the welded joint

Figure 2 shows the effect of the welding speed on the shape and microstructure of butt joints of AZ91 alloy. From the images it is evident that the width of the fusion zone is greater when the welding speed was very low. This indicates that the size of the weld pool increases with decreasing welding speed. Excessive melting of the base metal may cause the molten metal to flow down. Hence the concavity at the face and convexity at the root of the welded joint. At higher welding speeds, the fusion zone of the butt joint was narrower and regular in shape because the molten metal filled the space between the AZ91 plates completely. The formation of gas porosity was largely dependent on the welding speed. The amount and size of pores (pore area fraction) reached a maximum when the welding was carried out at a speed of 2.4 – 2.6 m/min (Fig. 2). The fusion zone was practically free from pores when the welding speed was 3.4 m/min, or higher.

Since the mechanical properties of welded joints can be greatly affected by porosity, the tests were continued at a safe speed of 3.4 m/min. The results of the microscopic analysis performed for the of AZ91 alloy welded joints at lower and higher magnifications are provided in Fig. 3 (left and right images, respectively). The material microstructure changes from the fusion zone (FZ) through the partially melted zone (PMZ) to the base material. The rapid loss of heat from the weld zone, where the material was liquid, to the surrounding base metal, which was solid, caused considerable dispersion of the structure constituents both in the FZ and in the PMZ. Very high magnification observations of the eutectic, which formed during the solidification of the laser melted metal, showed that its morphology was typical of a partially divorced eutectic. This type of eutectic is characterised by islands of a eutectic solid solution of aluminium in magnesium within the eutectic $Mg_{17}Al_{12}$ phase. The microstructure of the PMZ varies in direction from the fusion zone boundary to the base material. The eutectic is observed very near the fusion zone (the second higher magnification image of the microstructure). This reveals that significant but incomplete metal melting took place in this area. The analysis of the microstructure of the remaining part of the PMZ suggests that it was mainly the particles of the eutectic $Mg_{17}Al_{12}$ phase and possibly small part of the α phase (solid solution of aluminium in magnesium) that were melted. The respective microstructures are shown in the third and fourth higher magnification images in Fig. 3. This result indicates that only the interdendritic spaces of the primary structure of AZ91 alloy were melted. The microstructure presented in the fourth higher magnification image in Fig. 3 indicates that the $Mg_{17}Al_{12}$ particles at the boundary between the PMZ and the base material are only partially melted. The microstructure of the base material zone is distinguished primarily by the lamellar structure of discontinuous precipitates (the last higher magnification image of the weld microstructure in Fig. 3).

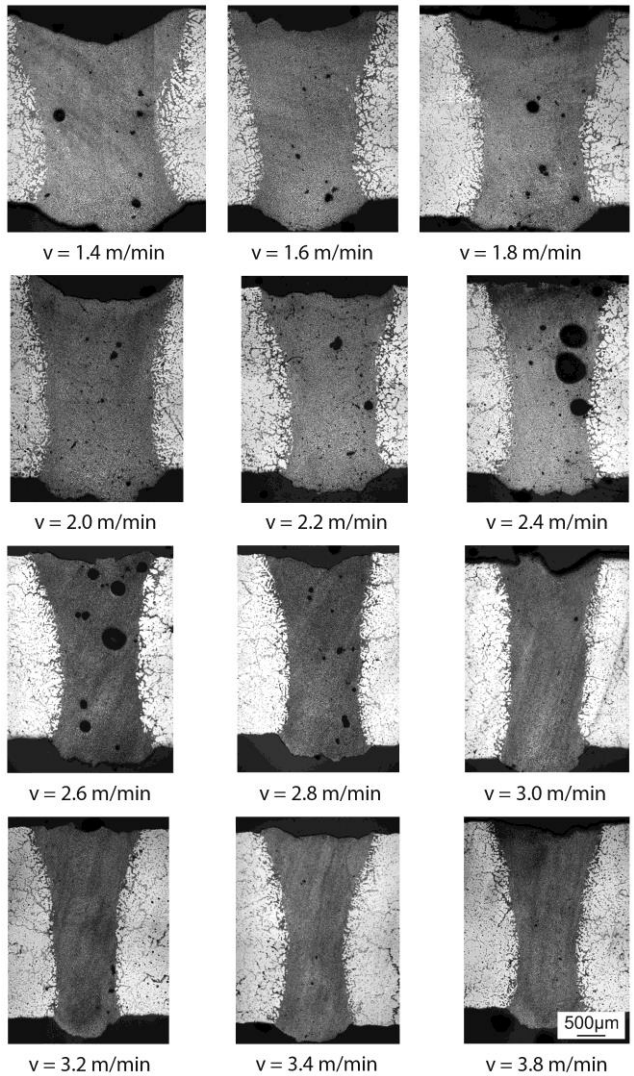

Fig. 2. Influence of the welding speed on the shape and porosity of butt joints of AZ91 alloy. Laser power: 2000 W

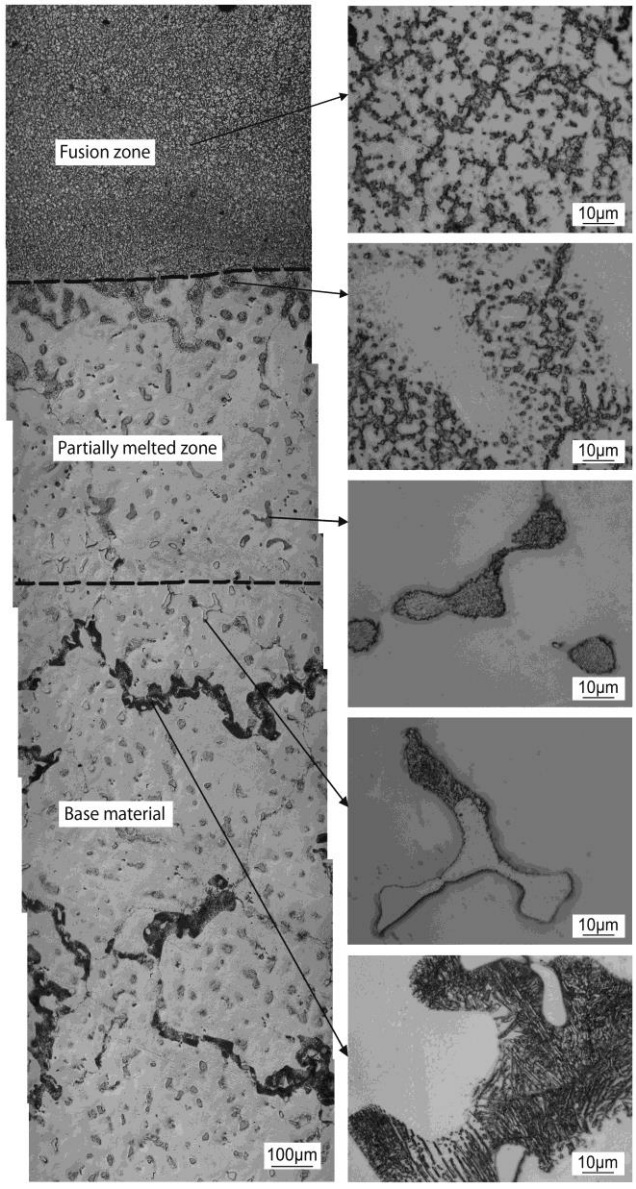

Fig. 3. Microstructure of the AZ91 alloy joint. Welding speed: 3.4 m/min

The microstructure of the material in the fusion zone obtained through SEM and the corresponding line scans for magnesium, aluminium and zinc are shown in Fig. 4. The results of the analysis indicate chemical heterogeneity in the spaces between the particles of the $Mg_{17}Al_{12}$-eutectic phase. The concentrations of Al and Zn are greater near the $Mg_{17}Al_{12}$ particles than in the area of dendrites. This result confirms earlier findings [20, 21] that the solid solution regions near the $Mg_{17}Al_{12}$ phase have a higher aluminium content compared to dendrite cores.

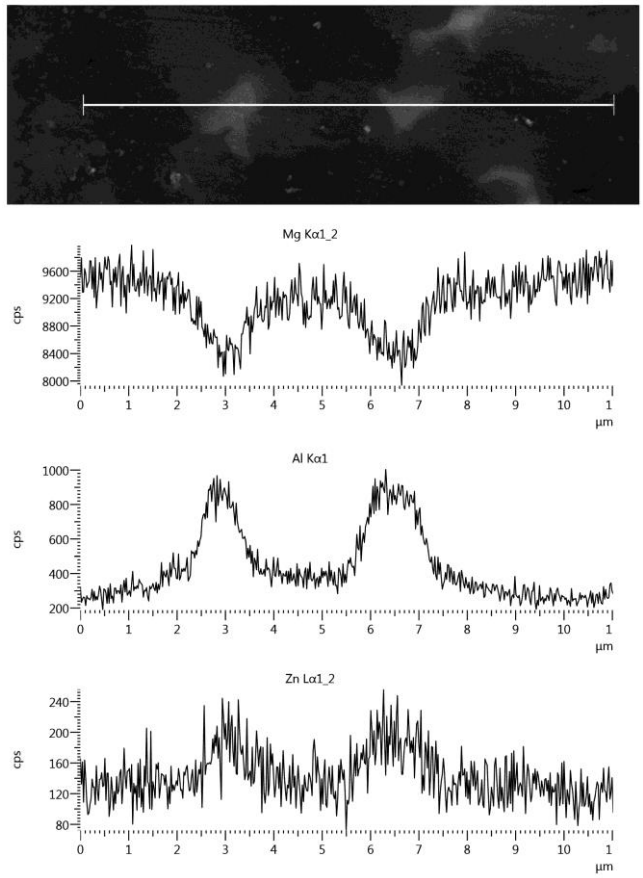

Fig. 4. SEM image of the microstructure of the fusion zone and the corresponding line scans for Mg, Al and Zn

3.3. Mechanical properties of the welded joint

The distribution of hardness in the cross-section of the welded joint is shown in Fig. 5. The hardness in the fusion zone was significantly higher than that in the base material.

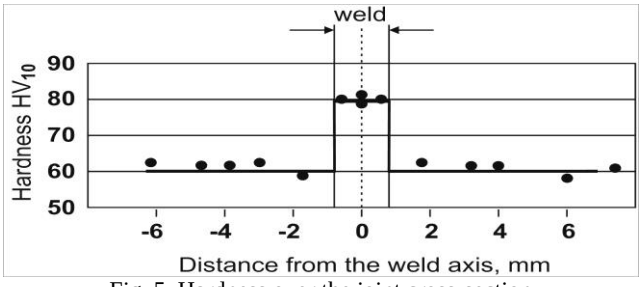

Fig. 5. Hardness over the joint cross-section

Table 1 shows the values of the yield strength, tensile strength and elongation obtained for the specimens with welded joints. Since the specimens cracked outside the weld, it should be assumed that the plastic deformation also occurred there. Thus, $R_{0.2,}$ calculated from the stress-strain curves plotted by the

universal testing machine, can be treated as the yield strength of the base material in the welded joint. The tensile properties were also determined for the as-cast, not welded AZ91 alloy. It should be added that the scatter of results was significant both in the group of welded and not welded samples. Table 1 gives the average values from four measurements for each group of samples.

Table 1.
Tensile properties of the AZ91 specimens

AZ91 alloy	Yield strength $R_{0.2}$ MPa	Tensile strength R_m MPa	Elongation A %
Welded	71	121	2.0
As-cast	63	120	2.0

All the welded specimens subjected to tensile tests fractured in the base material outside the fusion zone (Fig. 6). For this reason, the tensile strength and elongation of the welded samples were similar to those reported for the as-cast AZ91 alloy.

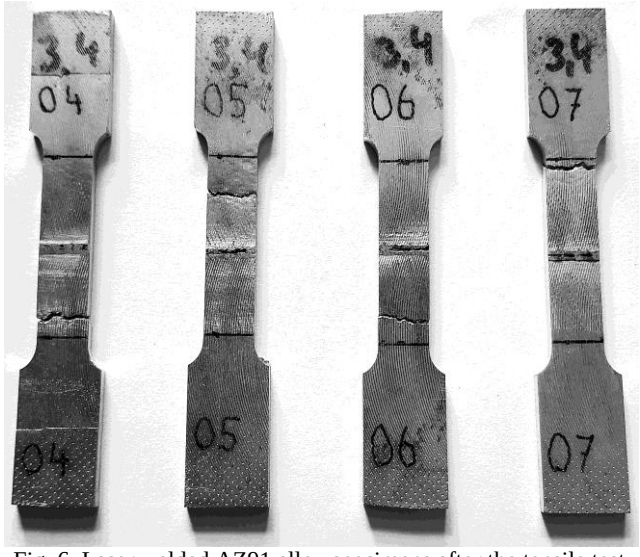

Fig. 6. Laser welded AZ91 alloy specimens after the tensile test

4. Discussion

The analysis of the literature shows that the most important laser welding parameters influencing the weld quality for magnesium alloys are laser power and welding speed. The findings of this study are similar to those provided by other researchers [12, 13, 15]. The width of the fusion zone decreases with increasing welding speed. However, it is difficult to compare the relationship between the porosity of the fusion zone and the welding speed described in this paper with those discussed by other researchers because, firstly, they performed the welding of AZ91 alloy using different types of laser (Nd : YAG), secondly, the joining was done at much higher welding speeds ranging from 4 to 10 m/min, and finally, a larger speed increment of about 1 m/min was used for the subsequent welding tests [14, 16]. As a result, the authors found that the volume fraction of porosity in the fusion zone decreased with welding speed. From the microstructure images in Fig. 2 it can be concluded that the weld porosity, which is treated here as the pore surface area per cross-sectional area of the fusion zone, reaches a maximum as a function of welding speed. A similar finding was reported only by Marya and Edwards [17] for the AZ91 alloy welded with a Nd : YAG laser using a power of 600 W. The pore area fraction was the highest at a welding speed of 0.24 to 0.30 m/min, which actually is an order of magnitude smaller than that obtained in this study. It seems that the phenomenon of porosity, which is affected by many factors related to the quality of the material welded and the welding process parameters [14], depends, to a large extent, on the type of laser applied.

The most important feature of the FZ microstructure is its refinement (Fig. 3). The degree of dispersion of the FZ microstructure is similar to that of the AZ91 alloy welded using the GTAW method [11] but much higher than that of the as-cast alloy formed in a cold steel mould [21]. Also, the rapid loss of heat between the fusion zone and the base material leads to the formation of a very narrow PMZ (about 0.8 mm). In this zone, the melting occurs predominately in the interdendritic regions of the base material except in the area adjacent to the FZ, where the dendrites of base material are also partially melted due to higher temperature. The microstructure of the non-molten base material is characterised primarily by the presence of lamellar discontinuous precipitates (last higher magnification image in Fig. 3).

The refinement of the microstructure (high dispersion of the $Mg_{17}Al_{12}$-eutectic phase) caused the hardness to increase to approx. 80 HV10 in the fusion zone, which was about 20 HV10 higher than the hardness of the as-cast AZ91 alloy. The strengthening of the FZ is not associated with its fragility; the tensile test results indicate that the welded specimens fractured in the base material. Thus, laser welding is suitable to produce joints that are not mechanically weaker than AZ91 cast alloy.

5. Conclusions

1. When the welding speed was increased from 1.4 to 3.8 m/min, the weld width was reduced by half. There was also a significant decrease in the face concavity.
2. The amount and size of pores were the highest when the welding process was carried out at a speed of 2.4 – 2.6 m/min and a laser power of 2000 W. The fusion zone was practically free from pores when the welding speed was 3.4 m/min, or higher.
3. The microstructure of the fusion zone is characterised by a high dispersion of $Mg_{17}Al_{12}$- eutectic particles. The partially melted zone is very narrow. The hardness of the fusion zone is about 20 HV10 higher than that of the base material.
4. All the welded specimens fractured outside the fusion zone, which suggests that the tensile strength of the welded joint was not lower than that of the base metal.

References

[1] Edgar,R.L. (2000). Global overview on demand and application for magnesium alloys. In International Congress "Magnesium Alloys and Their Applications", 26-28 September 2000 (pp. 3-8). Munich, Germany: Wiley-Vch Verlag.

[2] Pan, F., Yang, M. & Chen, X. (2016). A review on casting magnesium alloys: modification of commercial alloys and development of new alloys. *Journal of Materials Science and Technology*. 32, 1211-1221.

[3] Luo, A. & Pekguleryus, M.O. (1994). Cast magnesium alloys for elevated temperature applications. *Journal of Materials Science*. 29, 5259-5271.

[4] Polmear, I.J. (1994). Magnesium alloys and applications. *Materials Science and Technology*. 10, 1-16.

[5] Neite, G., Kubota, K., Higashi, K. & Hehmann, F. (2005). Magnesium-based alloys. In R. W. Cahn, P. Haasen, E. J. Kramer (eds.). *Materials Science and Technology*. 8/9, 113-212. Wiley-Vch. Verlag.

[6] Regev, M., Aghion, E., Rosen, A. & Bamberger, R. (1998). Creep studies of coarse-grained AZ91D magnesium castings. *Materials Science and Engineering* A. 252, 6-16.

[7] Song, G., Bowles, A.L. & StJohn, D.H. (2004). Corrosion resistance of aged die cast magnesium alloy AZ91D. *Materials Science and Engineering* A. 366, 74-86.

[8] Munitz A., Cotler C., Stern A. & Kohn, G. (2001). Mechanical properties and microstructure of gas tungsten arc welded magnesium AZ91D plates. *Materials Science and Engineering* A. 302, 68-73.

[9] Zhu, T., Chen, Z.W. & Gao, W. (2006). Incipient melting in partially melted zone during arc welding of AZ91D magnesium alloy. *Materials Science and Engineering* A. 416, 246-252.

[10] Shen, J., You, G., Long, S. & Pan, F. (2008). Abnormal macropore formation during double-sided gas tungsten arc welding of magnesium AZ91 alloy. *Materials Characterization*. 59, 1059-1065.

[11] Braszczyńska-Malik, K.N. & Mróz, M. (2011). Gas tungsten arc welding of AZ91 magnesium alloy. *Journal of Alloys and Compounds*. 509, 9951-9958.

[12] Marya, M. & Edwards, G.R. (2001). Factors controlling the magnesium weld morphology in deep penetration welding by a CO2 laser. *Journal of Materials Engineering and Performance*. 10, 435-443.

[13] Dhahri, M., Masse, J.E., Mathieu J.F., Barreau, G. & Autric, M. (2001). Laser welding of AZ91 and WE43 magnesium alloys for automotive and aerospace industries. *Advanced Engineering Materials*. 3, 504-507.

[14] Cao, X., Jahazi, M., Immarigeon, J.P. & Wallace, W. (2006). A review of laser welding techniques for magnesium alloys. *Journal of Materials Processing Technology*. 171, 188-204.

[15] Abderrazak, K., Salem, W.B., Mhiri, H., Bournot, P. & Autric, M. (2009). Nd:YAG Laser Welding of AZ91 magnesium alloy for aerospace industries. *Metallurgical and Materials Transactions* B. 40, 54-61.

[16] Wahba, M., Mizutani, M., Kawahito, Y. & Katayama, S. (2012). Laser welding of die-cast AZ91D magnesium alloy. *Materials and Design*. 33, 569-576.

[17] Marya, M. & Edwards, G.R. (2000). The laser welding of magnesium alloy AZ91. *Welding in the World*. 44, 31-37.

[18] Kouadri, A. & Barrallier, L. (2011). Study of Mechanical Properties of AZ91 magnesium alloy welded by laser process taking into account the anisotropy microhardness and residual stresses by X-Ray diffraction. *Metallurgical and Materials Transactions* A. 42, 1815-1826.

[19] Predel, B. (1998). Landolt-Börstein - Group IV physical chemistry (Numerical data and functional relationships in science and technology). Berlin: Springer-Verlag.

[20] Dahle, A.K., Lee, Y.C., Nave, M.D,. Schaffer, P.L. & StJohn, D.H. (2001). Development of the as-cast microstructure in magnesium-aluminium alloys. *Journal of Light Metals*. 1, 61-72.

[21] Dziadoń, A., Bucki, T. & Porzucek, P. (2018). The effect of non-equilibrium solidification on the structure and mechanical properties of AZ91 alloy. *Archives of Foundry Engineering*. 18(3), 120-125.